New Journal of Physics
The open-access journal for physics

Hydrogen-mediated ferromagnetism in ZnO single crystals

M Khalid[1,4], P Esquinazi[1], D Spemann[2], W Anwand[3] and G Brauer[3]

[1] Division of Superconductivity and Magnetism, University of Leipzig, D-04103 Leipzig, Germany
[2] Division of Nuclear Solid State Physics, University of Leipzig, D-04103 Leipzig, Germany
[3] Institut für Strahlenphysik, Forschungszentrum Dresden-Rossendorf, PO Box 510119, D-01314 Dresden, Germany
E-mail: m.khalid@physik.uni-leipzig.de

New Journal of Physics **13** (2011) 063017 (7pp)
Received 23 December 2010
Published 9 June 2011
Online at http://www.njp.org/
doi:10.1088/1367-2630/13/6/063017

Abstract. We investigated the magnetic properties of hydrogen-plasma-treated ZnO single crystals by using superconducting quantum interferometer device magnetometry. In agreement with the expected hydrogen penetration depth, we found that ferromagnetic behavior is present in the first 20 nm of the H-treated surface of ZnO with magnetization at saturation up to 6 emu g^{-1} at 300 K and a Curie temperature of $T_c \gtrsim 400$ K. In the ferromagnetic samples, a hydrogen concentration of a few atomic per cent in the first 20 nm of the surface layer was determined by nuclear reaction analysis. The saturation magnetization of H-treated ZnO increases with the concentration of hydrogen.

After a large number of studies and different kinds of efforts, experimental and theoretical work of the last few years indicates that defect-induced magnetism remains key to triggering ferromagnetism in ZnO (as well as in other non-magnetic oxides) with a Curie temperature above 300 K. It is not doping with magnetic elements that appears to be a successful and reproducible method to trigger magnetic order in this oxide, but the introduction of a certain defect density of the order of a few per cent, such as O [1] or Zn vacancies [2] with or without doping with non-magnetic ions such as C [3], N [4], Li [5] or Cu [6, 7]. In general, however, the achieved magnetization values are still too low, indicating that the magnetic order is most

[4] Author to whom any correspondence should be addressed.

probably not homogeneously distributed in the whole sample, a necessary condition for the application of this phenomenon in ZnO-based devices.

What about the influence of hydrogen in the magnetism of ZnO? It is known that the presence of hydrogen is unavoidable in all systems and in general it is still rather difficult to measure it with a high enough accuracy. Hydrogen-related magnetic order was recently found in graphite surfaces by x-ray magnetic circular dichroism [8], indicating that this element can play a role in the magnetism of nominally non-magnetic materials. The role of hydrogen in ZnO can be diverse. It can act either as a donor (H^+) or as an acceptor (H^-) and can even modify the host structure. In bulk ZnO, hydrogen acts as a shallow donor and is a source of unintentional *n*-type conductivity [9]. Room temperature ferromagnetism due to atomic hydrogen adsorption in different terminated surfaces of ZnO [10–12] or in the bulk of Co-doped ZnO [13] has been studied theoretically. In one of these studies, it was shown that atomic hydrogen adsorbed on the Zn plane on the ZnO(0001) surface forms strong H–Zn bonds, leading to a metallic surface with a net magnetic moment [12]. All these theoretical studies indicate that it is important to check whether hydrogen implantation can trigger ferromagnetism in ZnO. In this work, we investigate the magnetic properties of ZnO single crystals treated with remote hydrogen plasma and demonstrate that a remarkable ferromagnetic signal with a large magnetization is present in a few nm of the H-treated surface of ZnO single crystals. Our finding opens up a simple and reproducible possibility to trigger magnetic order in broad or localized regions of ZnO bulk, thin films or microstructures without the need to introduce other elements or vacancies.

Hydrothermally grown ZnO single crystals were used in hydrogen-plasma (H-plasma) treatment. Two of them were one-side polished (O-terminated) and of dimensions $\sim (10 \times 10 \times 0.5)\,\mathrm{mm}^3$ (MaTeck GmbH, Jülich). One of them was treated with H-plasma, whereas the other was kept as the reference. Both single crystals were cut before treatment to directly mount them in a straw in order to carry out magnetic measurements with a superconducting quantum interferometer device (SQUID). Four other crystals were two-side polished with similar termination but were of dimensions $\sim (6 \times 6 \times 0.5)\,\mathrm{mm}^3$ (CrysTec GmbH, Berlin). Hydrogen doping in ZnO can be achieved by, e.g., the adsorption of hydrogen on the ZnO surface, H implantation or remote H-plasma doping [14–16]. We used the last method to implant hydrogen into ZnO.

There are several parameters that may influence the strength of the magnetic order triggered through H-plasma treatment: namely, the sample temperature, the H^+-ion energy and current and the total implanted charge. In this work, we demonstrate how the substrate temperature and total implanted charge influence magnetic ordering in ZnO crystals. The substrate temperature was varied from room temperature to 400 °C, whereas the total implanted charge was controlled by varying the treatment time from 30 to 90 min. The ZnO surface was placed $\sim$100 nm downstream of the plasma with a bias voltage of ~ -330 V (the parallel-plate system with a voltage difference of 10^3 V). The bias current was fixed at $\sim 50\,\mu$A (the sample plus the sample holder), while the current flowing into the sample was only nA. The exposure to remote hydrogen dc plasma ranges from 30 to 90 min. During the loading the gas pressure was $\sim$1 mbar.

The hydrogen content before and after H-treatment was determined by standard nuclear reaction analysis (NRA) [17] using 6.64 MeV ^{15}N ions with a depth resolution of $\sim$5 nm and a H detection limit of $\sim$200 ppm. The H-concentration versus depth was obtained using SRIM (stopping and range of ions in matter) simulation [18]; see figure 1. The average hydrogen atomic concentration of bound hydrogen measured by NRA within the top 100 nm of the

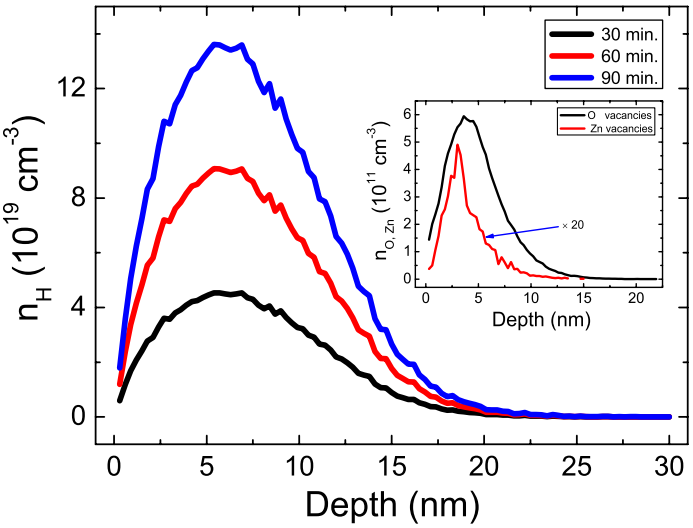

Figure 1. The hydrogen concentration versus penetration depth of H^+ ions in ZnO single crystals at different total implanted times, estimated by SRIM. The simulation results show that most of the H^+ ions are implanted within the first 20 nm of the surface. The inset shows the concentration of oxygen and zinc vacancies produced in ZnO single crystals during 90 min H implantation under the energy conditions used.

surface region of ZnO crystals before and after a 60 min treatment was (0.14 ± 0.03) and (0.64 ± 0.07) at.%, respectively. Comparable results were reported recently [19]. The average H-concentration reached in the 20 nm surface region after 60 min implantation in the present conditions was $\sim 2.5 \pm 0.5$ at.%. Particle-induced x-ray emission measurements were used to analyze the magnetic impurities of the samples before and after H treatment. There was no significant difference in magnetic impurity concentration between the samples before and after H-plasma treatment.

Several ZnO single crystals were treated with H-plasma. All of them showed an increase in ferromagnetic moment after H-plasma treatment, compared to their as grown values. The increase in ferromagnetic moment depends on the temperature of the sample during H-treatment at nominally similar total implanted charge. Figure 2 shows the saturation values of the ferromagnetic magnetization signal (after the subtraction of the diamagnetic linear background) for several samples treated with H-plasma for 90 min at different temperatures. We found that ferromagnetic saturation magnetization increases with increasing sample temperature and reaches a maximum at 350 °C. Therefore, we concentrate on the study of samples implanted at 250 and 350 °C. We note that the observed dependence on the sample temperature might be very useful in controlling H diffusion as well as lattice defects produced both during and after plasma treatment.

In what follows, we discuss the results for samples treated at 350 and 250 °C with a 1 h implantation and the results for samples implanted at 350 °C but with a different total charge (or implantation time). The results shown in this paper were found to be unaffected by aging after the samples were kept for 1 year at 300 K.

Figure 3 shows the magnetic moment at 300 K of a H–ZnO single crystal treated at 350 °C and at applied magnetic fields parallel and perpendicular to the main sample area.

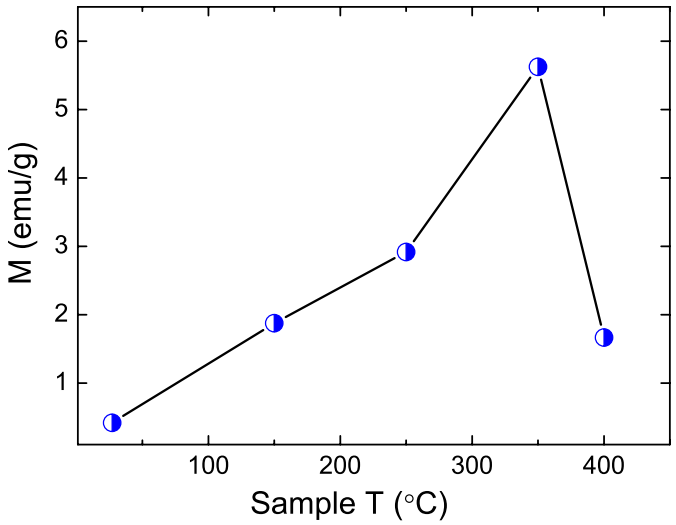

Figure 2. Room temperature saturation magnetization of the ferromagnetic signal of H–ZnO single crystals treated at different substrate temperatures, all with similar nominally implanted charge.

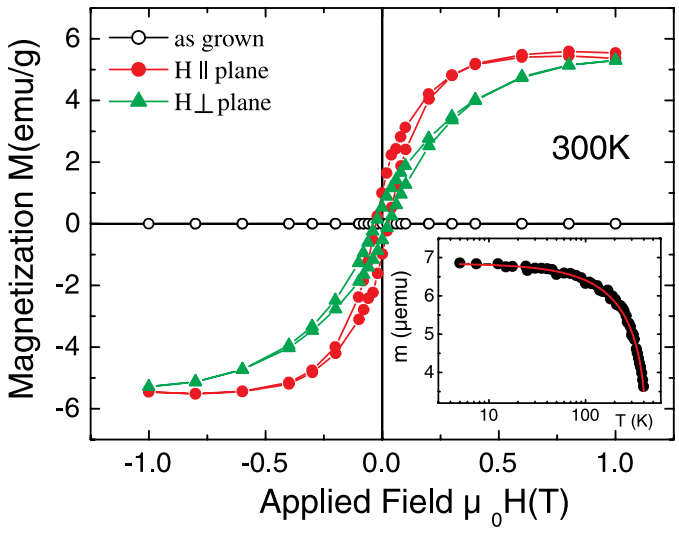

Figure 3. Hysteresis loops of a H–ZnO single crystal measured at 300 K by applying magnetic fields parallel (●) and perpendicular (▲) to the main plane of the sample. The open circles (○) represent the ferromagnetic magnetization of the untreated ZnO crystal, calculated by taking into account the whole volume of the sample. The diamagnetic linear background was subtracted from the measured signal. The inset shows the remanent moment versus temperature. The (red) solid line is given by $m(T) = 6.8[\mu\text{emu}](1 - T/T_c)^{1/3})$ with a Curie temperature of $T_c = 450$ K.

Clear ferromagnetic hysteresis loops are observed at 300 K. The ferromagnetic behavior of the hysteresis shows a clear magnetocrystalline anisotropy with an anisotropy constant $K_1 \sim 2 \times 10^5\,\text{J m}^{-3}$. This anisotropy also excludes magnetic impurities as the origin of the observed ferromagnetism. The remanent magnetic moment versus temperature shown in the

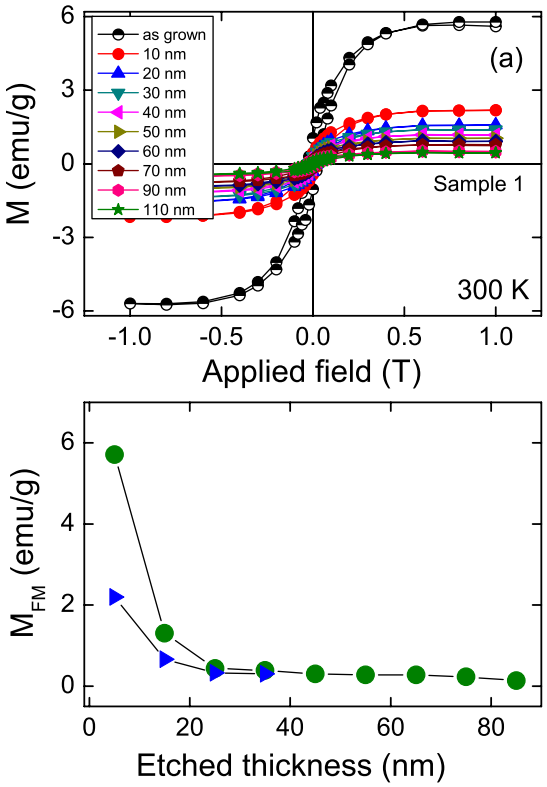

Figure 4. (a) The magnetic moment as a function of applied magnetic field for a H–ZnO single crystal at different etching stages, after subtraction of the diamagnetic contribution at 300 K. (b) Ferromagnetic magnetization values at saturation obtained taking into account the change in magnetic moment (see (a)) after etching a specific thickness of the surface region for H-treated samples at substrate temperatures of 350 °C (•) and 250 °C (▲).

inset of figure 3 was measured at zero field after applying a field parallel to the sample main surface and cooled down in the field to 5 K. The temperature dependence of the remanence follows $m(T) = m_0(1 - T/T_c)^{\delta}$ with $\delta = 0.33 \pm 0.05$, a static scaling law with an exponent similar to other ferromagnets such as $CrBr_3$ [20]. This fit indicates a Curie temperature of $T_c = 450 \pm 25$ K.

In order to investigate how much thickness of the surface of ZnO single crystals contributes to the observed ferromagnetism, we etched up to ∼100 nm thick layer and studied the change in ferromagnetic moment. For this purpose, we used a solution of 0.3 ml of HCl in 400 ml of water [21, 22]. The single crystals were etched from both sides and then the measured etched mass was divided by 2 to exclude the mass of the H-untreated side. After ≃40 s etching time, ≃4 μg mass of the ZnO crystal was removed, which means a ≃10 nm thick layer from the H-treated side. After etching a 10 nm thick layer the hysteresis loop was measured at 300 K. These results are shown in figure 4(a). Knowing the etched mass and the corresponding change in ferromagnetic moment, we can calculate the real magnetization of the H-treated layer. The magnetization as a function of etched thickness for two samples treated at different temperatures is shown in figure 4(b). From these results, it becomes clear that the major ferromagnetic contribution vanishes after etching the top ≃ 20 nm layer, a layer thickness

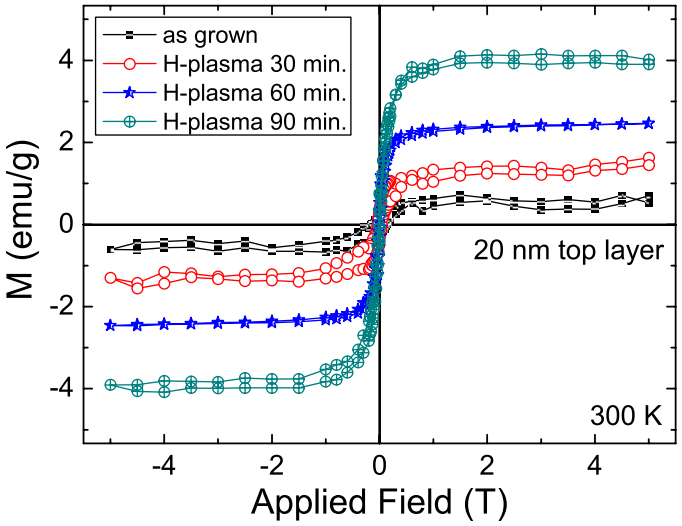

Figure 5. Magnetization of H–ZnO single crystals versus applied field measured at different total implantations. The saturation magnetization increases with increasing implanted charge.

that agrees with the H-concentration calculated using SRIM and shown in figure 1. At the H^+-energies used, the estimated concentration of O and Zn vacancies is eight and nine orders of magnitude smaller than the H-concentration in the first 20 nm of the surface; see the inset in figure 1. This huge difference clearly indicates that in the treated samples, it is hydrogen at a concentration of several per cent at the surface and not Zn or O vacancies or interstitials that plays a major role in the observed magnetic order.

We also studied the influence on the ferromagnetic signal of the amount of hydrogen implanted into the sample. The samples were treated with H-plasma at a temperature of 350 °C for three different total implanted times: 30, 60 and 90 min. The ferromagnetic signals of these samples are shown in figure 5. For comparison, the ferromagnetic magnetization of an untreated ZnO single crystal, calculated by taking the first 20 nm surface layer, is also shown. We observe that the magnetization of H–ZnO crystals increases with the total treatment time.

Using the measured ferromagnetic magnetization within the first 20 nm surface region, we estimate a magnetic moment of the order of $0.2\mu_B$ per ZnO unit cell. If we assume that on average about one H atom per unit cell exists in this 20 nm region, then this magnetic moment triggered by each H atom is comparable to that obtained in [12].

In conclusion, we have investigated the magnetic properties of remote H-plasma-treated ZnO single crystals. The NRA results confirmed the enhanced concentration of hydrogen in ZnO single crystals after treatment. Characteristic ferromagnetic hysteresis loops as well as magnetic anisotropy were observed in H–ZnO samples at room temperature. Systematic measurements of the magnetic moment of the treated samples carried out after wet chemical etching proved that only the $\lesssim$20 nm-thick surface layer of H-treated ZnO contributes to the total ferromagnetic magnetization, in agreement with the expected H-penetration depth estimated by SRIM. We attribute the observed ferromagnetism in H–ZnO single crystals to the influence of hydrogen. Because hydrogen implantation also reduces dramatically the resistivity of the ZnO structure, this ferromagnetic oxide should be more easily applicable in spintronic devices. Magnetotransport measurements on similar H-treated samples are currently being

carried out. We have observed the anomalous Hall effect, anisotropic magnetoresistance (AMR) and a negative magnetoresistance in H-ZnO crystals. The anomalous Hall effect signals match quantitatively those from SQUID magnetization measurements. The magnitude of the AMR effect at 250 K is $\sim 0.5\%$ of the measured resistance at a field of 5 T. The existence of an AMR in H-ZnO crystals indicates a finite LS coupling as well as a spin asymmetry in the electronic band structure. These results will be published elsewhere [23].

Acknowledgment

This work was supported by the DFG within the Collaborative Research Center (SFB 762) 'Functionality of oxide interfaces'.

References

[1] Banerjee S, Mandal M, Gayathri N and Sardar M 2007 *Appl. Phys. Lett.* **91** 182501
[2] Khalid M *et al* 2009 *Phys. Rev.* B **80** 035331
[3] Zhou S *et al* 2008 *Appl. Phys. Lett.* **93** 232507
[4] Wu K Y, Fang Q Q, Wang W N, Zhou C, Huang W J, Li J G, Lv Q R, Liu Y M, Zhang Q P and Zhang H M 2010 *J. Appl. Phys.* **108** 063530
[5] Chawla S, Jayanthi K and Kotnala R K 2009 *Phys. Rev.* B **79** 125204
[6] Xu Q *et al* 2008 *Appl. Phys. Lett.* **92** 082508
[7] Yi J B *et al* 2010 *Phys. Rev. Lett.* **104** 137201
[8] Ohldag H, Esquinazi P, Arenholz E, Spemann D, Rothermel M, Setzer A and Butz T 2010 *New J. Phys.* **12** 123012
[9] Van de Walle C G 2000 *Phys. Rev. Lett.* **85** 1012
[10] Wang C, Zhou G, Li J, Yan B and Duan W 2008 *Phys. Rev.* B **77** 245303
[11] Woll C 2007 *Prog. Surf. Sci.* **82** 55
[12] Sanchez N, Gallego S, Cerda J and Munoz M C 2010 *Phys. Rev.* B **81** 115301
[13] Liu E-Z, Liu J-F, He Y and Jiang J Z 2009 *J. Magn. Magn. Mater.* **321** 3507
[14] Torbrugge S, Ostendorf F and Reichling M 2009 *J. Phys. Chem.* C **113** 4909
[15] Wang D F, Lu H B, Li J C, Wu Y, Tian Y and Lee Y P 2009 *Mater. Res. Bull.* **44** 41
[16] Strzhemechny Y M *et al* 2004 *Appl. Phys. Lett.* **84** 2545
[17] Lanford W A 1995 *Handbook of Modern Ion Beam Materials Analysis* ed R Tesmer and M Nastasi (Pittsburgh, PA: Materials Research Society)
[18] Ziegler J F, Biersack J P and Littmark U 1985 *The Stopping and Range of Ions in Solids* (New York: Pergamon)
[19] Anwand W, Brauer G, Cowan T E, Grambole D, Skorupa W, Čižek J C, Kuriplach J, Procházka I, Egger W and Sperr P 2010 *Phys. Status Solidi* a **207** 2415
[20] John T and Ho Litster J D 1970 *Phys. Rev.* B **2** 4523–32
[21] Maki H, Ikoma T, Sakaguchi I, Ohashi N, Haneda H, Tanaka J and Ichinose N 2002 *Thin Solid Films* **411** 91
[22] Lin T T and Lichtman D 1977 *J. Appl. Phys.* **48** 2164
[23] Khalid M and Esquinazi P 2011 to be published